

## SUPPORTING INFORMATION

# Crude-Oil-Repellent Membranes by Atomic Layer

## Deposition: Oxide Interface Engineering

*Hao-Cheng Yang<sup>1</sup>, Yunsong Xie<sup>2</sup>, Henry Chan<sup>1</sup>, Badri Narayanan<sup>1</sup>, Lin Chen<sup>2</sup>, Ruben Z. Waldman<sup>3</sup>,  
Subramanian K. R. S. Sankaranarayanan<sup>1,4</sup>, Jeffrey W. Elam<sup>2,4</sup>, and Seth B. Darling<sup>\*1,3,4</sup>*

<sup>1</sup> Center for Nanoscale Materials, Argonne National Laboratory, Lemont, IL, 60439, USA

<sup>2</sup> Energy Systems Division, Argonne National Laboratory, Lemont, IL, 60439 USA

<sup>3</sup> Institute for Molecular Engineering, University of Chicago, Chicago, IL, 60637, USA

<sup>4</sup> Institute for Molecular Engineering, Argonne National Laboratory, Lemont, IL, 60439, USA

**Table S1** ALD precursors used for the different oxides.

Oxide	Precursor A	Precursor B
ZnO	Diethyl zinc (DEZ)	H <sub>2</sub> O
Al <sub>2</sub> O <sub>3</sub>	Trimethyl aluminum (TMA)	H <sub>2</sub> O
TiO <sub>2</sub>	Titanium tetrachloride (TTC)	H <sub>2</sub> O
SnO <sub>2</sub>	Tetrakis(dimethylamino) tin(IV) (TDMASn)	H <sub>2</sub> O

**Table S2** ALD cycle numbers, growth rate, and thickness of different oxides

Oxide	ALD cycles	Thickness (nm)*	Growth rate ( $\text{\AA}/\text{cyc}$ )
ZnO	58	$9.8 \pm 0.13$	1.69
$\text{Al}_2\text{O}_3$	77	$9.5 \pm 0.15$	1.23
$\text{TiO}_2$	100	$10.6 \pm 0.12$	1.06
$\text{SnO}_2$	78	$10.2 \pm 0.11$	1.28

\* Thickness of oxide layers measured on silicon wafers, which may differ from that on membranes.

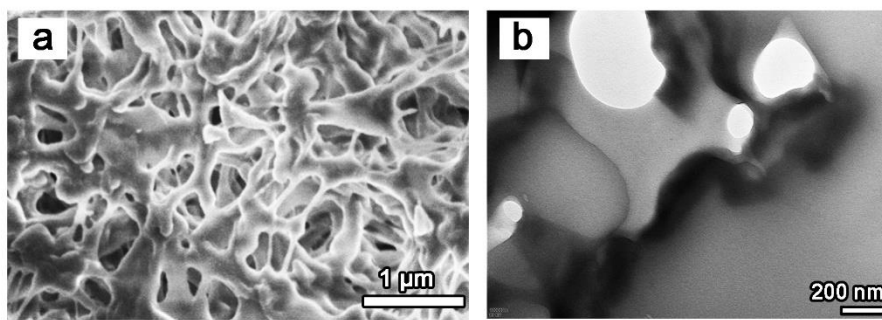


**Figure S1.** a) SEM and b) TEM images of the nascent PVDF membrane

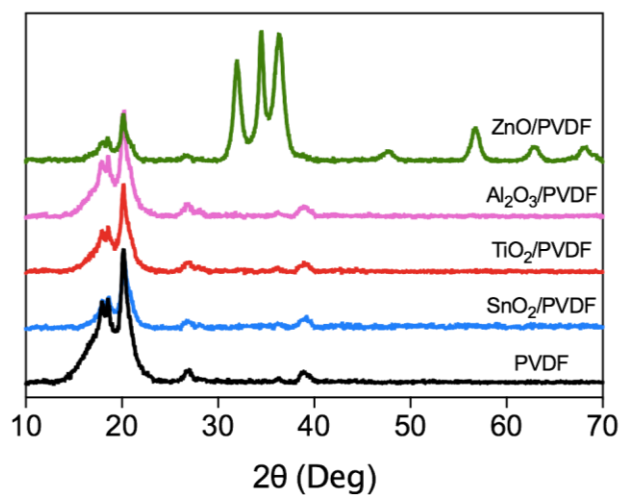


**Figure S2.** XRD spectra of nascent and oxide-coated membranes

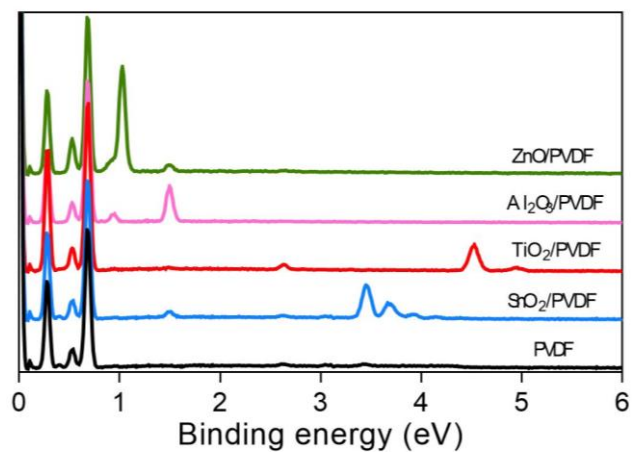


**Figure S3.** EDS spectra of membranes

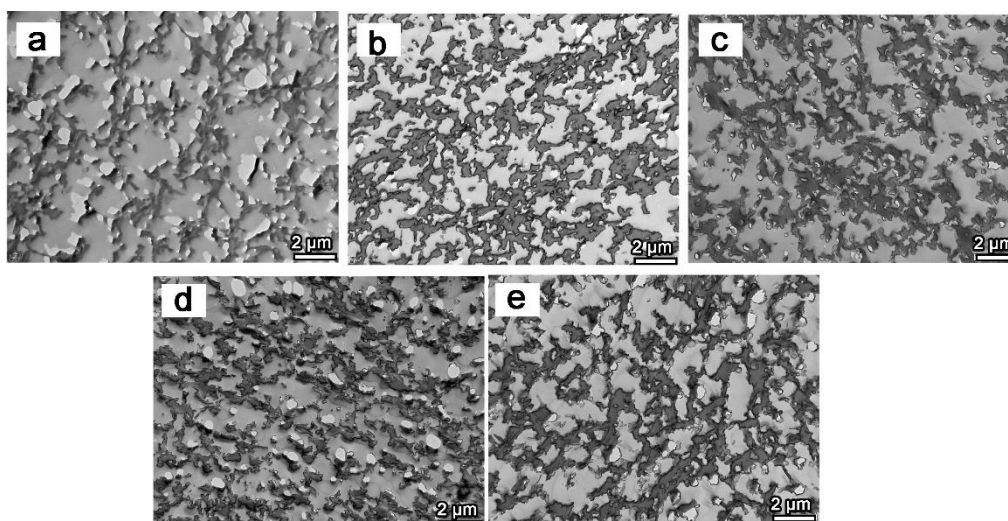


**Figure S4.** TEM images of the slices of a) nascent, b) ZnO-coated, c) Al<sub>2</sub>O<sub>3</sub>-coated, d) TiO<sub>2</sub>-coated, and e) SnO<sub>2</sub>-coated membranes at low magnification.

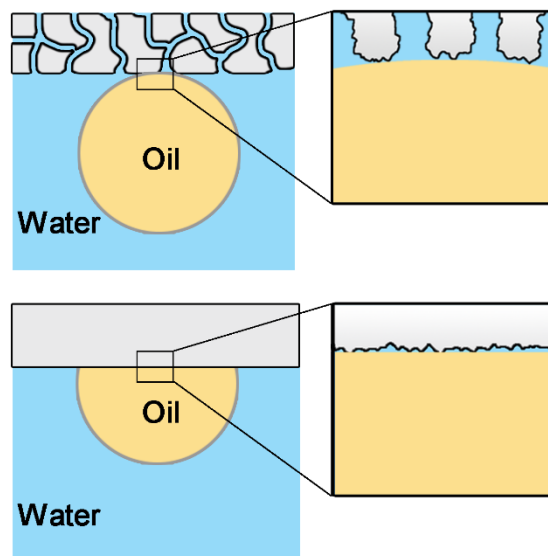


**Figure S5.** Scheme of the oil contact angles on membrane and silicon water surfaces. Despite minimal roughness on the silicon surface, it can be also regarded as an ideal “composite surface” for an adhesion work calculation.

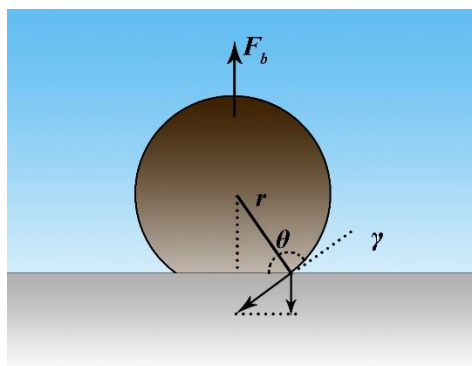


**Figure S6** Force analysis of oil on a membrane surface under water. As shown in Figure SX,  $F_b$  is the buoyancy,  $\gamma$  is the counterforce of surface tension acting on oil by the membrane surface,  $\theta$  is the oil contact angle, and  $r$  the radius of the oil droplet. The lifting fore is the buoyancy  $F_b \approx \rho g \frac{4}{3} \pi r^3$ , while the adhesion force is  $F_a = 2\pi r \gamma \sin^2 \theta$ , which achieves a balance when  $F_a = F_b$ . We can conclude from these equations that the adhesion force can be reduced by increasing the oil contact angle and decreasing the contact area/triple phase line.



**Figure S7.** Crude oil in permeate solution in the case of nascent PVDF membrane

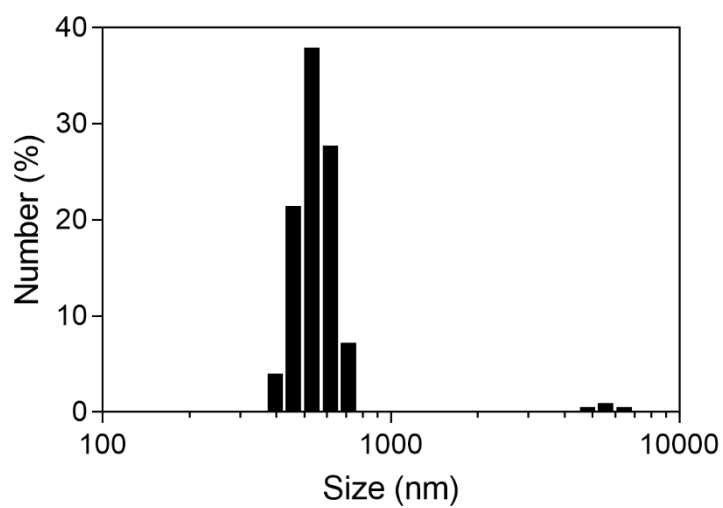


**Figure S8** Size distribution of oil droplets in oil/water mixture. The permeate shows no peaks.